



Prediction of MCI to AD conversion, via MRI, CSF biomarkers, and pattern classification

AQ: 1

Christos Davatzikos^{a,*}, Priyanka Bhatt^a, Leslie M. Shaw^{b,c}, Kayhan N. Batmanghelich^a, John Q. Trojanowski^{b,c}

^a Section of Biomedical Image Analysis, Department of Radiology, University of Pennsylvania, Philadelphia, PA, United States

^b Department of Pathology and Laboratory Medicine, University of Pennsylvania, Philadelphia, PA, United States

^c Center for Neurodegenerative Disease Research, Department of Pathology and Laboratory Medicine, University of Pennsylvania, Philadelphia, PA, United States

Received 8 January 2010; received in revised form 4 May 2010; accepted 17 May 2010

Abstract

AQ: 2

Magnetic resonance imaging (MRI) patterns were examined together with cerebrospinal fluid (CSF) biomarkers in serial scans of Alzheimer's Disease Neuroimaging Initiative (ADNI) participants with mild cognitive impairment (MCI). The SPARE-AD score, summarizing brain atrophy patterns, was tested as a predictor of short-term conversion to Alzheimer's disease (AD). MCI individuals that converted to AD (MCI-C) had mostly positive baseline SPARE-AD (Spatial Pattern of Abnormalities for Recognition of Early AD) and atrophy in temporal lobe gray matter (GM) and white matter (WM), posterior cingulate/precuneus, and insula. MCI individuals that converted to AD had mostly AD-like baseline CSF biomarkers. MCI nonconverters (MCI-NC) had mixed baseline SPARE-AD and CSF values, suggesting that some MCI-NC subjects may later convert. Those MCI-NC with most negative baseline SPARE-AD scores (normal brain structure) had significantly higher baseline Mini Mental State Examination (MMSE) scores (28.67) than others, and relatively low annual rate of Mini Mental State Examination decrease (-0.25). MCI-NC with midlevel baseline SPARE-AD displayed faster annual rates of SPARE-AD increase (indicating progressing atrophy). SPARE-AD and CSF combination improved prediction over individual values. In summary, both SPARE-AD and CSF biomarkers showed high baseline sensitivity, however, many MCI-NC had abnormal baseline SPARE-AD and CSF biomarkers. Longer follow-up will elucidate the specificity of baseline measurements.

© 2010 Elsevier Inc. All rights reserved.

Keywords: Alzheimer's disease; Early detection; Mild cognitive impairment; MCI; Pattern classification; Imaging biomarkers; CSF biomarkers; SPARE-AD

1. Introduction

The incidence of Alzheimer's disease (AD) doubles every 5 years after the age of 65, rendering the disease the major cause for dementia as well as a very important health and socioeconomic issue, particularly in view of increasing life expectancy (Bain et al., 2008; Hebert et al., 2001). Although most currently approved treatments are symptomatic and don't directly slow AD pathology progression, it is

anticipated that new disease-modifying treatments will be available in the near future. It is also expected that treatment decisions will greatly benefit from diagnostic and prognostic tools that identify individuals likely to progress to dementia sooner. This is especially important in individuals with mild cognitive impairment (MCI), who present a conversion rate of approximately 15% per year.

Two promising and potentially complementary biomarkers of early AD are structural changes measured by magnetic resonance imaging (MRI), and cerebrospinal fluid (CSF) concentrations of $A\beta_{42}$, a marker that tends to correlate inversely with amyloid plaque deposition in the brain, and tau protein, a marker of neuronal injury that correlates with neurofibrillary tangles. A number of studies have re-

* Corresponding author at: Department of Radiology, University of Pennsylvania, 3600 Market Street, Suite 380, Philadelphia, PA 19104, United States. Tel.: +1 215 349 8587; fax: +1 215 614 0266.

E-mail address: christos@rad.upenn.edu (C. Davatzikos).

ported relatively reduced brain volumes in the hippocampus, parahippocampal gyrus, cingulate, and other brain regions in both MCI and AD patients (Chetelat et al., 2002; Convit et al., 2000; De Leon et al., 2006; Dickerson et al., 2001; Fox and Schott, 2004; Jack et al., 1999, 2008; Karas et al., 2004; Kaye et al., 1997; Killiany et al., 2000; Penanen et al., 2005; Risacher et al., 2009; Stoub et al., 2005; Thompson et al., 2007; Visser et al., 2002). Studies using CSF biomarkers have also shown the promise of CSF tau and A β 42 measures as diagnostic tests for AD as well as potential predictors of risk for developing AD in normal individuals and those with MCI (Hampel et al., 2010a, 2010b; Schuff et al., 2009; Shaw et al., 2009).

The spatial patterns of brain atrophy in MCI and AD are complex and highly variable, depend on the stage of the disease, and are concurrent with structural changes occurring with normal aging not necessarily being associated with clinical progression (Driscoll et al., 2009; Resnick et al., 2003). Advanced pattern analysis and classification methods have been found in recent years to be promising tools for capturing such complex spatial patterns of brain structure (Davatzikos et al., 2009; Duchesne et al., 2008; Fan et al., 2008b; Gerardin et al., 2009; Hinrichs et al., 2009; Kloppel et al., 2008; Lao et al., 2004; McEvoy et al., 2009; Vemuri et al., 2009). Importantly, these methods have begun to provide tests of high sensitivity and specificity on an individual patient basis, in addition to characterizing group differences, hence they can potentially be used as diagnostic and prognostic tools. Herein, we use a marker termed SPARE-AD (Spatial Pattern of Abnormalities for Recognition of Early AD), which has been found in previous studies to be a good predictor of MCI to AD conversion (Misra et al., 2009), but also of conversion from normal cognition to MCI in healthy elderly individuals (Davatzikos et al., 2009). This marker was also found to be a good differential diagnostic marker between AD and frontotemporal dementia (FTD) (Davatzikos et al., 2008b). As a primary goal in this study, we investigate the SPARE-AD individually, and in combination with CSF biomarkers, aiming to utilize information from baseline measurements in order to predict MCI individuals likely to convert to AD in a relatively short period (the average follow-up period in this study was 12 months). The secondary goal of this study is to measure the spatial pattern of brain atrophy, as well as its longitudinal change, in MCI converters (MCI-C) and in

MCI nonconverters (MCI-NC) in the Alzheimer's Disease Neuroimaging Initiative (ADNI) cohort, and to evaluate differences between these 2 groups. The hypothesis was that pattern analysis and classification techniques applied to images of the regional distribution of brain tissues, in conjunction with CSF biomarkers, would allow us to predict future conversion from MCI to AD.

2. Methods

2.1. Participants

ADNI participants of this study include 239 MCI patients, whose preprocessed baseline and follow-up examinations we had downloaded from the ADNI web site by April 2009 (see below) and were available in our database. Data from the MCI patients were followed for an average period of approximately 12 months with a standard deviation of 6 months (range: 6–36 months). According to their Clinical Dementia Rating (CDR) scores during the follow-up period, MCI subjects were divided into 2 subgroups: converters (MCI-C), whose diagnosis was MCI at baseline and their global CDR score changed from CDR = 0.5 to CDR = 1, and nonconverters, whose global CDR score remained stable. For this study, we had considered 69 MCI-C; and 170 MCI-NC. We also used a previously reported high-dimensional pattern classifier that determines the SPARE-AD score (Fan et al., 2008a), which had been trained on data from 63 cognitively normal (CN) individuals and 54 AD patients, all ADNI participants. Table 1 provides more details about the sample.

2.2. MRI acquisition

The datasets included standard T1-weighted images obtained using volumetric 3-dimensional magnetization prepared rapid acquisition gradient echo (MPRAGE) or equivalent protocols with slightly varying resolutions. For this study only those scans were considered which had gone through certain correction methods such as gradwarp, B1 calibration, N3 correction, and (in-house) skull-stripping. Detailed information about magnetic resonance (MR) acquisition procedures is available at the ADNI web site (www.loni.ucla.edu/ADNI/) and in (Jack et al., 2008).

AQ:3

AQ:4

T1

AQ:8

Table 1
Number of Subjects, Average Age, Sex, Average Baseline MMSE Scores, and APOE Status for AD, CN, MCI-C, and MCI-NC Groups

	AD	CN	MCI-C	MCI-NC
Subjects, <i>n</i>	54	63	69	170
Average age	77.4 \pm 7.10	75.2 \pm 5.40	76.9 \pm 6.88	74.5 \pm 7.35
Sex (male/female)	23 M, 31 F	33 M, 30 F	39 M, 30 F	103 M, 67 F
Average MMSE	23.2 \pm 2.10	29.2 \pm 0.98	25.8 \pm 2.18	27.1 \pm 1.82
Percentage having 1 and 2 APOE4 alleles, respectively	48%, 22%	27%, 5%	46%, 16%	38%, 11%

Key: AD, Alzheimer's disease; APOE, apolipoprotein E; CN, cognitively normal; MCI-C, mild cognitive impairment individuals that converted to AD; MCI-NC, mild cognitive impairment individuals that did not convert to AD; MMSE, Mini Mental State Examination.

2.3. Collection and analysis of CSF biomarkers

Baseline CSF samples were obtained in the morning following an overnight fast from ADNI subjects enrolled at 56 participating centers at the time the subjects entered ADNI. Their demographic, clinical and *APOE* genotyping results are comparable to that in the full ADNI patient population. Lumbar puncture was performed with a 20-gauge or 24-gauge spinal needle as described in the ADNI procedures manual (www.adni-info.org/ADNIStudyProcedures/LumbarPunctures.aspx) and in Shaw et al. (2009). Written informed consent was obtained for participation in these studies, as approved by the Institutional Review Board (IRB) at each participating center. $A\beta_{1-42}$, total tau (t-tau) and tau phosphorylated at residue 181 (p-tau_{181p}) were measured in each of the 416 CSF ADNI baseline aliquots using the multiplex xMAP Luminex platform (Luminex Corp, Austin, TX) with Innogenetics (INNO-BIA AlzBio3, Ghent, Belgium; for research use only reagents) immunoassay kit-based reagents as described by Shaw et al. (2009). Prior to performing these analyses of the ADNI CSF samples in the University of Pennsylvania ADNI Biomarker Core Laboratory, an interlaboratory study was conducted in order to qualify the performance conditions, including all major variables that can affect the test results, for the immunoassay reagents and analytical platform. The findings from these studies provided the basis for achieving day-to-day reproducibility for the 3 biomarkers of <10% variation for CSF pool samples and <7% for aqueous quality controls. Only subjects with a valid test result for all 3 biomarkers are included in this study, as described in Shaw et al. (2009). The diagnostic thresholds for each of the CSF biomarkers were established using premortem CSF samples from ADNI-independent patients who were followed to autopsy to establish a postmortem diagnosis of AD and age-matched living cognitively normal subjects (Shaw et al., 2009).

2.4. Image analysis

The images were processed with previously used and published pipeline (Goldszal et al., 1998). The first step was rigid alignment to the *anterior commissure - posterior commissure (ac-pc)* plane, followed by semiautomated removal of skull and cerebellum tissues. The images were then segmented into 4 tissue types: gray matter (GM), white matter (WM), sulcal CSF, and ventricles (VN). These segmented images were registered to the common brain atlas (Kabani et al., 1998) using high dimensional image warping to create tissue density maps for GM, WM, and ventricles. These maps are also called RAVENS maps. The RAVENS maps are the results of elastic registration of original brain regions to the standard template while preserving the original tissue volumes. Therefore, regional volumetric measurements and comparisons are performed via measurements and comparisons of the respective RAVENS maps. For example, patterns of GM atrophy in the temporal lobe are quantified by patterns of RAVENS decrease in the temporal lobe in the template space. The RAVENS ap-

proach has been extensively validated and applied to a variety of studies and is similar to the “modulated by the Jacobian voxel-based morphometry (VBM)” approach. RAVENS maps were normalized for intracranial volume, in order to account for head size variations.

2.5. Statistical analysis and pattern classification

The normalized RAVENS maps were smoothed using 8 mm full-width at half-maximum (FWHM) Gaussian smoothing kernel. For measuring the rate of progression of atrophy, “beta” maps were created by applying voxel-wise linear regression to RAVENS maps of subjects with at least 2 follow-up scans. The group analyses were done on baseline RAVENS maps as well as on beta maps. To display significantly different regions between two MCI groups, voxel-wise *t* tests were performed using SPM software (www.fil.ion.ucl.ac.uk/spm/software/spm5).

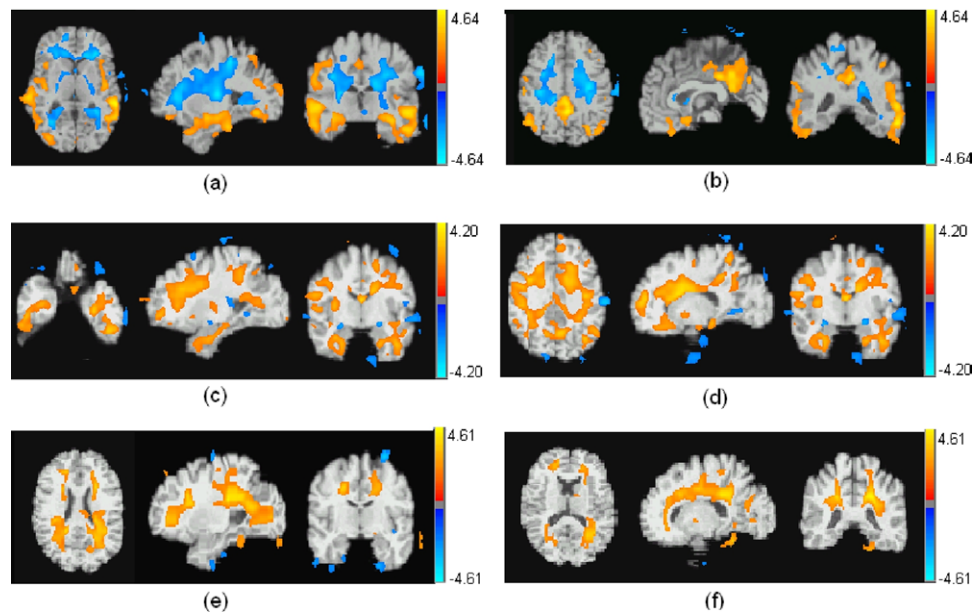
With the aim to provide abnormality scores for individual MCI subjects, we utilized a high dimensional pattern classification method (Fan et al., 2007). This method looks for the combination of brain regions, which can form a unique pattern that maximally differentiates between 2 groups. This classifier was trained in (Fan et al., 2008a) on the AD and CN subjects; it provides an output that tends to be close to +1 for AD patients and -1 for CN subjects. This classifier was applied to all (baseline and follow-up) scans of the MCI patients, yielding a SPARE-AD score for each scan. Positive SPARE-AD scores indicated more AD-like characteristics and vice-versa.

3. Results

3.1. Group comparisons via voxel-based analysis

The voxel-by-voxel analysis between 2 MCI subgroups showed significant reduction of GM and WM in MCI-C compared with MCI-NC, at baseline. The results are shown in Fig. 1. Several regions of relatively reduced volumes of GM in MCI-C compared with MCI-NC are evident (red/yellow colors), including the hippocampus, amygdala, and entorhinal cortex, much of the temporal lobe GM, and the insular cortex (especially the superior temporal gyrus), posterior cingulate and precuneus, and orbitofrontal cortex. Regions of increased periventricular WM tissue that appears gray, likely due to more pronounced leukoaraiosis in MCI-C, relative to MCI-NC, were also evident and are shown in Fig. 1a and b (blue colors), potentially indicating relatively more pronounced small-vessel disease in the former group. In agreement with this was the reduced WM in the periventricular frontal region which is shown in Fig. 1c and d (red/yellow colors). WM was also relatively reduced in MCI-C in the perihippocampal temporal lobe region.

As discussed in the methods section, we also looked at group differences of the “beta” maps, i.e., of the rate of longitudinal change of brain tissue. The only findings were in GM RAVENS maps, and are displayed in Fig. 1e and f. The most



AQ: 9 Figure 1. Maps of the t statistics showing differences between mild cognitive impairment (MCI) individuals that converted to Alzheimer's disease (AD) (MCI-C) and nonconverters (MCI-NC). (a and b) Significantly more gray matter (GM) in MCI-NC relative to MCI-C (red/yellow), and areas of relatively increased periventricular white matter (WM) tissue that appears gray in T1 images, likely due to leukoaraiosis, in MCI-C relative to MCI-NC (blue). (c and d) Regions of relatively reduced WM in MCI-C relative to MCI-NC (red/yellow). Temporal, prefrontal, and orbitofrontal reduced WM are evident, along with periventricular loss likely due to leukoaraiosis, and with white matter in the vicinity of the precuneus. (e and f) The difference in rate of GM change over time ("beta" maps) between MCI-C and MCI-NC. Red/yellow reflects relatively more rapidly increasing gray-looking tissue in MCI-C, likely due to progression of leukoaraiosis. Regions of relatively higher loss of GM tissue in MCI-C are shown in blue, reflecting higher rate of atrophy in MCI-C. Images are in radiology convention. T-maps were thresholded at the $p = 0.05$ level.

pronounced group difference in these beta maps was in the higher rate of periventricular leukoaraiosis. Increased temporal cortical and anterior hippocampal atrophy was also measured.

The SPARE-AD scores of the AD and CN individuals were found to be in the expected range (mostly positive for the former and negative for the latter), therefore reconfirming the SPARE-AD as a marker of AD structural patterns. The average SPARE-AD scores were 0.69 ± 0.50 and -0.80 ± 0.43 for AD and CN groups, respectively, while they were 0.65 ± 0.44 and 0.22 ± 0.74 for MCI-C and MCI-NC. The histograms of the SPARE-AD scores of MCI-C and MCI-NC are

shown in Fig. 2. Most MCI-C had positive scores, in fact their range of SPARE-AD values were indistinguishable from AD patients (t test revealed no statistically significant differences), suggesting that significant atrophy has already occurred at MCI, for the people who are bound to convert to AD within the time frame of this study. SPARE-AD scores of about 1 third of the MCI-NC, however, were completely normal, indicating that a subgroup of MCI has normal brain structure, and that this subgroup does not convert to AD in the time frame of this study. However a majority of MCI-NC had sharply positive SPARE-AD scores, indicat-

F2

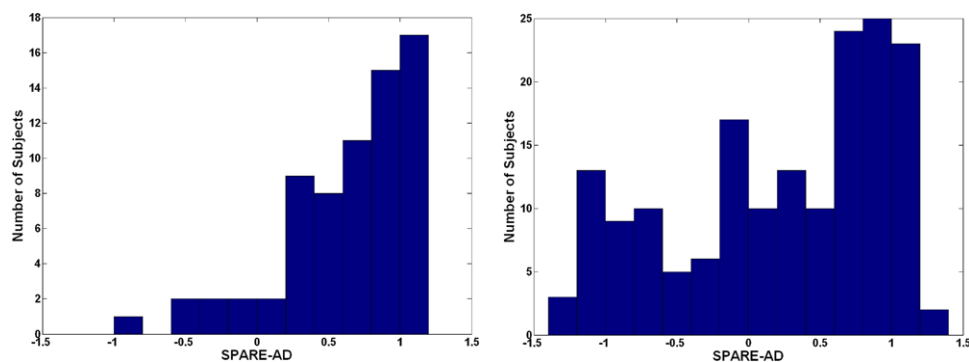


Figure 2. The histograms of baseline SPARE-AD (Spatial Pattern of Abnormalities for Recognition of Early AD) scores for mild cognitive impairment (MCI) individuals that converted to Alzheimer's disease (AD) (MCI-C) (left) and nonconverters (MCI-NC) (right).

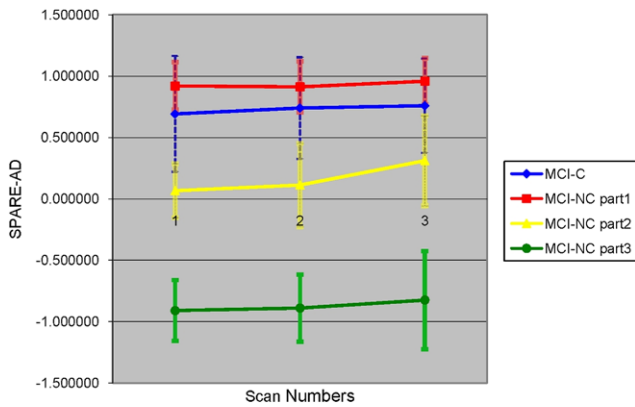


Figure 3. Trajectories of average SPARE-AD scores for mild cognitive impairment (MCI) individuals that converted to Alzheimer's disease (AD) (MCI-C) and subgroups of nonconverters (MCI-NC). Scan 3 is on the average 12 months after scan 1.

ing significant atrophy similar to AD patients and to MCI-C. Voxel-based group comparison (images not shown) between the subgroup of MCI-NC with positive SPARE-AD scores and MCI-C showed a picture similar to Fig. 1a and b. Future follow-ups will determine whether these individuals convert or remain stable.

The MCI-NC patients seemed to comprise 3 groups: people with low scores (well into the negative range centered around -1), people with scores around 0 (borderline cases), and people with high scores (well into the positive range centered around $+1$). We examined the longitudinal trajectories of these 3 subgroups separately, by obtaining SPARE-AD scores of all follow-ups. We used the following 3 ranges to subdivide the MCI-NC: SPARE-AD scores > 0.5 (part 1), SPARE-AD scores between -0.5 and 0.5 (part 2), and SPARE-AD scores below -0.5 (part 3). The average baseline and follow-up SPARE-AD scores are shown in Fig. 3, along with the trajectory of the average SPARE-AD score of the MCI-C group.

3.2. Integration of SPARE-AD and CSF in MCI

We only had a complete set of SPARE-AD and CSF biomarker measurements for a subset of 120 MCI patients with follow-up. Fig. 4 jointly plots the CSF biomarkers data with SPARE-AD scores for MCI subjects. In order to evaluate the predictive value of combinations of imaging and CSF biomarkers, we used the Weka software (www.cs.waikato.ac.nz/ml/weka/), with input that features the SPARE-AD and various CSF biomarkers. A linear support vector machine (SVM) (Vapnik, 1998) was used in a 5-fold cross-validation framework (20% of the data was left out, training was performed on the rest, and testing on the left-out patients; this procedure was repeated 5 times, with a different set of patients left out each time). The resulting classification accuracies and area under the curve (AUC) measures are shown in Table 2. For the SPARE-AD, we also repeated this experiment on all 239 patients (recall that we had CSF and SPARE-AD values for only a subset of 120 patients, whereas we had SPARE-AD values for all 239 patients).

In order to graphically show the joint value of SPARE-AD and CSF biomarkers, in Fig. 4 we plot the SPARE-AD against CSF tau and $A\beta_{42}$. In the same plots we include 2 SVM classifiers determined for different levels of sensitivity (by varying the cost of misclassification of MCI-C relative to MCI-NC, one can create many such SVM separating lines, each of which corresponds to a different point on the receiver operating characteristic (ROC) curve).

4. Discussion

We present a study here of 239 MCI patients from the ADNI cohort. Pattern analysis and classification were used to: (1) examine the spatial distribution of atrophy and small vessel disease; and (2) to derive a classification score, the SPARE-AD, whose predictive value at baseline was measured relative to future clinical progression. We first summarize and discuss the main findings of this study.

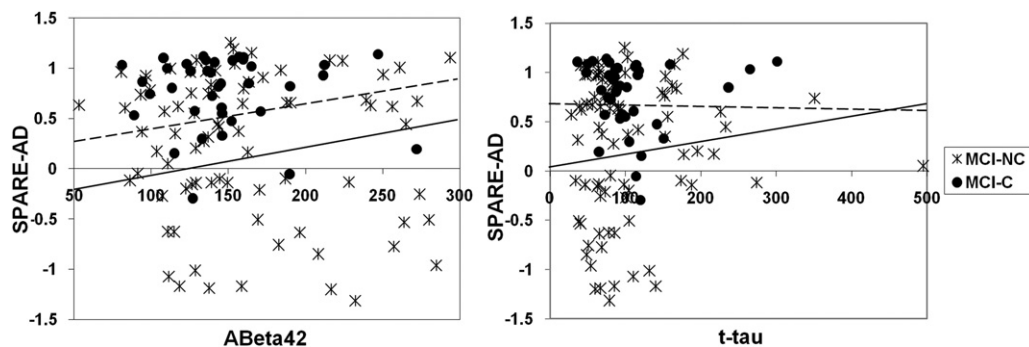


Figure 4. Scatterplots of SPARE-AD against cerebrospinal fluid (CSF) markers $A\beta_{42}$ and total tau (t-tau). The 2 oblique lines represent the support vector machine (SVM) classifiers achieving 2 different levels of sensitivity, i.e., correct classification of mild cognitive impairment (MCI) individuals that converted to Alzheimer's disease (AD) (MCI-C): $\sim 82\%$ (dotted line) and $\sim 92\%$ (solid line).

F4

T2,
AQ: 5

AQ: 6

F3

Table 2
Classification of MCI-C Versus MCI-NC

	Sensitivity (%)	Specificity (%)	Classification rate (%)	AUC
SPARE-AD	94.7 (89.8)	37.8 (37.0)	55.8 (52.3)	0.734 (0.660)
SPARE-AD and t-tau	84.2	51.2	61.7	0.677
SPARE-AD and A β 42	84.2	50.0	60.8	0.671
SPARE-AD and t-tau and A β 42	84.2	50.0	60.8	0.671
SPARE-AD and t-tau/A β 42	84.2	50.0	60.8	0.671
SPARE-AD and p-tau	81.6	51.2	60.8	0.664
SPARE-AD and p-tau _{181P} /A β 42	81.6	50.0	60.0	0.658
t-tau	47.4	61.0	56.7	0.595
LR-TAA model	84.2	29.3	46.7	0.579
t-tau/A β 42	86.8	35.4	51.7	0.564
p-tau _{181P}	76.3	33.0	46.7	0.551
p-tau _{181P} /A β 42	89.5	23.2	44.2	0.548
t-tau and A β 42	78.9	30.5	45.8	0.547
A β 42	89.5	24.4	45.0	0.545

Sensitivity is the proportion of mild cognitive impairment individuals that converted to Alzheimer's disease (MCI-C) correctly classified, and specificity is the proportion of mild cognitive impairment individuals that did not convert to Alzheimer's disease (MCI-NC) correctly classified, based on their baseline scores. Parentheses show the predictive value of the SPARE-AD score alone, when evaluated on the entire sample of 239 MCI patients; the rest of the numbers are from a subset of 120, for which both CSF and SPARE-AD values were available.

Key: AUC, area under the curve; LR-TAA, ; p-tau, phosphorylated tau; SPARE-AD, Spatial Pattern of Abnormalities for Recognition of Early AD; t-tau, total tau.

4.1. Spatial patterns of atrophy

The spatial pattern of structural differences between MCI-C and MCI-NC were quite extensive, and included temporal lobe GM and WM, posterior cingulate and precuneous, insula, and periventricular abnormal WM (presumably due to small vessel disease). Moreover, a somewhat surprising finding was that the most pronounced difference in rate of structural change was the faster progression of gray regions around the ventricles, which are hypothesized to reflect small vessel disease. Faster medial and inferior temporal lobe atrophy was also measured in MCI-C, but was far less pronounced. These findings emphasize the complexity and spatial extent of the patterns of brain atrophy that characterize brain structure in MCI and that, together with advanced pattern analysis and recognition methods, are likely to provide powerful imaging markers for diagnosis, as well as for prediction and quantification of disease progression. Moreover, these findings could potentially emphasize the importance of cerebrovascular disease, as well as its rate of change, in predicting future clinical progression. Although cerebrovascular disease has been shown to be a comorbid pathology in AD patients that contributes to dementia (Schneider et al., 2004), it has not received as much attention in the field of AD compared with hippocampal and temporal lobe atrophy. Unfortunately, the ADNI protocol does not include fluid attenuated inversion recovery (FLAIR) images, which usually provide better tissue contrast for measurement of vascular lesions. However, the T1-based measurements used in this study, in conjunction with the voxel-based analysis which localized the gray tissue increases around the ventricles, highlight the need for more in-depth investigations of the role of leukoaraiosis and cerebrovascular disease in AD.

4.2. Predictive value of SPARE-AD

The SPARE-AD score, which is derived from high-dimensional pattern classification algorithms, was found to have very good sensitivity, in that almost all MCI-C patients had positive or near-positive scores at baseline. Not unexpectedly, specificity was limited. This is largely due to the short follow-up of this study, which is a limitation of the current study that we anticipate to address in future analyses. Because MCI patients convert to AD at a rate of approximately 15% annually, it is anticipated that many MCI-NC will convert to AD in the near future. Although future studies with longer follow-up times will refine our estimates of specificity, our results indicated that positive SPARE-AD scores in MCI-NC were associated with faster Mini Mental State Examination (MMSE) decline. This was especially evident in the part 1 subgroup of MCI-NC, i.e., the subgroup with the highest baseline SPARE-AD scores, which showed an MMSE change around -0.9 annually. In contrast, the other 2 parts of the MCI-NC group showed significantly slower cognitive decline. Although average MMSE decline rates for MCI-NC part 1 and MCI-NC part-2/3 were markedly different, there was no statistical significance, largely due to their broad range (see Table 3). Importantly, although part 2 and part 3 of the MCI-NC group showed relatively comparable rates of MMSE decline, the former showed notably more rapid increase of the SPARE-AD score. This implies that a midrange baseline SPARE-AD score predicts faster future atrophy, yet not very different cognitive decline compared with the low baseline SPARE-AD score group (part 3). However, it is also important to emphasize that the baseline MMSE scores of part 3 were considerably higher than those of part 2 (and of the remaining groups). One possible hypothesis would

Table 3

Average Values of SPARE-AD, Age, Baseline MMSE, and Rate of Change of MMSE Along with APOE Status for MCI-C and 3 Subgroups of MCI-NC

	Average SPARE-AD	Average age	Average baseline MMSE scores	Average rate of change of MMSE per year	Percentage having 1 and 2 APOE4 alleles, respectively
MCI-C	0.69	77.5 ± 8.51	26.5	-2.0 ± 2.32	44,16
MCI-NC part 1 (SPARE-AD > 0.5)	0.92	75.6 ± 6.30	26.9	-0.9 ± 2.19	48,10
MCI-NC part 2 (-0.5 < SPARE-AD < 0.5)	0.07	73.0 ± 6.48	26.7	-0.3 ± 1.60	46,14
MCI-NC part 3 (SPARE-AD < -0.5)	-0.90	68.5 ± 8.84	28.7	-0.3 ± 1.53	15,15

Key: APOE, apolipoprotein E; MCI-C, mild cognitive impairment individuals that converted to Alzheimer's disease; MCI-NC, mild cognitive impairment individuals that did not convert to Alzheimer's disease; MMSE, Mini Mental State Examination; SPARE-AD, Spatial Pattern of Abnormalities for Recognition of Early AD.

then be that, if during earlier years before this study part 2 and part 3 had declined at similar rates to the rates measured herein, a period several years of this differential decline (-0.3 vs. -0.25) would be necessary to build up to the significant MMSE differences at baseline (26.71 vs. 28.67). Recent results from a longitudinal study of normal aging showed faster but gradual increase of the SPARE-AD score in individuals that converted from cognitively normal to MCI (Davatzikos et al., 2009). These results suggest that gradual brain changes over long periods might eventually lead to clinical progression to MCI. Imaging biomarkers that capture these patterns of brain change are therefore likely to provide useful tools for very early diagnosis, but also for quantifying treatment effects early.

4.3. Integration of SPARE-AD and CSF biomarkers

The CSF biomarkers showed comparable, yet slightly lower predictive value, compared with SPARE-AD. In particular, A β 42 as well as the ratio of t-tau and p-tau over A β 42 showed very high sensitivity in predicting conversion to AD, but low specificity. The explanation is likely to be the same as the explanation for the performance of SPARE-AD: many of the MCI-NC are likely to become MCI-C in the near future while some also are likely to progress to dementia due to causes other than AD. The combination of CSF biomarkers and the SPARE-AD had some additive value, relative to each biomarker individually, although this relationship was not very strong. Longer follow up of these ADNI subject, including postmortem confirmation of their underlying neuropathology, is likely to clarify how these imaging and chemical biomarkers relate to underlying disease processes as well as the potential resilience of individuals to different burdens of neurodegenerative disease. Our results are in general agreement with previous studies using analogous models (Vemuri et al., 2009). In addition to using a different methodology, which was trained on clinical AD patients instead of autopsy-defined AD and used different feature selection methods, the current study also reports sensitivity, specificity, and classification accuracy for individuals, as opposed to the study in Vemuri et al., 2009, which used linear statistical models to investigate the general relationship between the Structural Abnormality Index

(STAND) and CSF scores, and conversion to AD. Although sensitivity and specificity are not reported in Vemuri et al., 2009, the sensitivity of the SPARE-AD score suggests that this index is clinically useful for identifying MCI-C. Future follow-up studies will further elucidate the longer term clinical outcome of the MCI-NC.

It is important to note that the SPARE-AD score tends to saturate at around +1. In other words, further increase in atrophy of individuals with a score +1 will no longer change their scores significantly. Put differently, if an individual has a full-blown pattern of atrophy seen in AD patients, his/her score is around +1, regardless of even higher levels of atrophy that he/she might develop. This is by construction of the SPARE-AD and increases our ability to better examine the range of patterns between normal and AD, which is the range that is clinically most interesting. Accordingly, the MCI-NC individuals in the part 1 subgroup are likely to lose additional brain tissue in the future, however, at this point their brains already have the full pattern of atrophy seen in AD patients. Their rapid change of MMSE score, coupled with the already significantly reduced baseline MMSE scores, indicate that these individuals are likely to soon convert to AD.

4.4. Role of white matter

Although the majority of the findings related to GM and periventricular leukoaraiosis, there was quite pronounced atrophy of WM surrounding the hippocampus and other temporal lobe structures. This indicates that more careful evaluations of WM integrity in early AD might further improve our ability to identify MCI individuals likely to convert to AD. Diffusion tensor imaging, as well as high angular resolution diffusion imaging (HARDI), are promising imaging protocols for evaluation of WM structure.

The majority of MCI-NC had positive SPARE-AD scores. Comparison of these individuals with MCI-C and with AD patients showed virtually no structural differences. This has important implications. In particular, it indicates that most MCI individuals have fully developed brain atrophy, even though they do not convert to AD in the time frame of this study. These individuals are therefore less likely to enjoy long term benefits from potential treatments, as would

be individuals at earlier stages of AD. Treatment trials therefore may be far more effective on cognitively normal elderly, provided that biomarkers such as the ones examined herein are proven to identify normal individuals likely to progress to MCI in the near future. Some recent studies have suggested that early changes of the SPARE-AD scores and other morphological measurements, as well as CSF biomarkers, in cognitively normal elderly are good predictors of future progression to MCI (Davatzikos et al., 2008a, 2008b, 2009; Driscoll et al., 2009; Fagan et al., 2009).

AQ:7 Disclosure statement

The authors disclose no actual or potential conflicts of interest.

Written informed consent was obtained for participation in these studies, as approved by the Institutional Review Board (IRB) at each participating center.

Acknowledgements

The authors thank Evi Parmpi for her help with handling MRI datasets.

Financial support was partially provided by grants R01AG14971, a grant by the Institute for the Study of Aging, AG-10124 and AG-024904.

Data used in the preparation of this article were obtained from the Alzheimer's Disease Neuroimaging Initiative (ADNI) database (www.loni.ucla.edu/ADNI). As such, the investigators within the ADNI contributed to the design and implementation of ADNI and/or provided data but did not participate in analysis or writing of this report. A complete listing of ADNI investigators is available at http://www.loni.ucla.edu/ADNI/Data/ADNI_Manuscript_Citations.doc.

References

- Bain, L.J., Jedrzewski, K., Morrison-Bogorad, M., Albert, M., Cotman, C., Hendrie, H., Trojanowski, J.Q., 2008. Healthy brain aging: A meeting report from the Sylvan M. Cohen Annual Retreat of the University of Pennsylvania Institute on Aging. *Alzheimers Dement.* 4, 443–446.
- Chetelat, G., Desgranges, B., de la Sayette, V., Viader, F., Eustache, F., Baron, J.-C., 2002. Mapping gray matter loss with voxel-based morphometry in mild cognitive impairment. *Neuroreport* 13, 1939–1943.
- Convit, A., de Asis, J., de Leon, M.J., Tarshish, C.Y., De Santi, S., Rusinek, H., 2000. Atrophy of the medial occipitotemporal, inferior, and middle temporal gyri in non-demented elderly predict decline to Alzheimer's disease. *Neurobiol. Aging* 21, 19–26.
- Davatzikos, C., Fan, Y., Wu, X., Shen, D., Resnick, S.M., 2008a. Detection of prodromal Alzheimer's disease via pattern classification of magnetic resonance imaging. *Neurobiol. Aging* 29, 514–523.
- Davatzikos, C., Resnick, S.M., Wu, X., Parmpi, P., Clark, C.M., 2008b. Individual patient diagnosis of AD and FTD via high-dimensional pattern classification of MRI. *Neuroimage* 41, 1220–1227.
- Davatzikos, C., Xu, F., An, Y., Fan, Y., Resnick, S., 2009. Longitudinal progression of Alzheimer's-like patterns of atrophy in normal older adults: the SPARE-AD index. *Brain* 132, 2026–2035.
- De Leon, M., DeSanti, S., Zinkowski, R., Mehta, P., Pratico, D., Segal, S., Rusinek, H., Li, J., Tsui, W., Louis, L.S., 2006. Longitudinal CSF and MRI biomarkers improve the diagnosis of mild cognitive impairment. *Neurobiol. Aging* 27, 394–401.
- Dickerson, B.C., Goncharova, I., Sullivan, M.P., Forchetti, C., Wilson, R.S., Bennett, D.A., Beckett, L.A., deToledo-Morrell, L., 2001. MRI-derived entorhinal and hippocampal atrophy in incipient and very mild Alzheimer's disease. *Neurobiol. Aging* 22, 747–754.
- Driscoll, I., Davatzikos, C., An, Y., Wu, X., Shen, D., Kraut, M., Resnick, S.M., 2009. Longitudinal pattern of regional brain volume change differentiates normal aging from MCI. *Neurology* 72, 1906–1913.
- Duchesne, S., Caroli, A., Geroldi, C., Barillot, C., Frisoni, G.B., Collins, D.L., 2008. MRI-Based Automated Computer Classification of Probable AD Versus Normal Controls. *IEEE Trans. Med. Imaging* 27, 509–520.
- Fagan, A.M., Head, D., Shah, A.R., Marcus, D., Mintun, M., Morris, J.C., Holtzman, D.M., 2009. Decreased cerebrospinal fluid Abeta(42) correlates with brain atrophy in cognitively normal elderly. *Ann. Neurol.* 65, 176–183.
- Fan, Y., Batmanghelich, N., Clark, C.M., Davatzikos, C., Alzheimer's Disease Neuroimaging Initiative, 2008a. Spatial patterns of brain atrophy in MCI patients, identified via high-dimensional pattern classification, predict subsequent cognitive decline. *Neuroimage* 39, 1731–1743.
- Fan, Y., Resnick, S.M., Wu, X., Davatzikos, C., 2008b. Structural and functional biomarkers of prodromal Alzheimer's disease: A high-dimensional pattern classification study. *Neuroimage* 41, 277–285.
- Fan, Y., Shen, D., Gur, R.C., Gur, R.E., Davatzikos, C., 2007. COMPARE: Classification Of Morphological Patterns using Adaptive Regional Elements. *IEEE Trans. Med. Imaging* 26, 93–105.
- Fox, N., Schott, J., 2004. Imaging cerebral atrophy: normal ageing to Alzheimer's disease. *Lancet* 363, 392–394.
- Gerardin, E., Chetelat, G., Chupin, M., Cuingnet, R., Desgranges, B., Kim, H.S., Niethammer, M., Dubois, B., Lehericy, S., Garnero, L., Eustache, F., Colliot, O., 2009. Multidimensional classification of hippocampal shape features discriminates Alzheimer's disease and mild cognitive impairment from normal aging. *Neuroimage* 47, 1476–1486.
- Goldszal, A.F., Davatzikos, C., Pham, D., Yan, M., Bryan, R.N., Resnick, S.M., 1998. An image processing protocol for the analysis of MR images from an elderly population. *J. Comput. Assist. Tomogr.* 22, 827–837.
- Hampel, H., Blennow, K., Shaw, L.M., Hoessler, Y.C., Zetterberg, H., Trojanowski, J.Q., 2010a. Total and phosphorylated tau protein as biological markers of Alzheimer's disease. *Exp. Gerontol.* 45, 30–40.
- Hampel, H., Shen, Y., Walsh, D.M., Aisen, P., Shaw, L.M., Zetterberg, H., Trojanowski, J.Q., Blennow, K., 2010b. Biological markers of amyloid beta-related mechanisms in Alzheimer's disease. *Exp. Neurol.* 223, 334–346.
- Hebert, L., Beckett, L., Scherr, P., Evans, D., 2001. Annual incidence of Alzheimer disease in the United States projected to the years 2000 through 2050. *Alzheimer Dis. Assoc. Disord.* 15, 169–173.
- Hinrichs, C., Singh, V., Mukherjee, L., Xu, G., Chung, M.K., Johnson, S.C., Alzheimer's Disease Neuroimaging Initiative, 2009. Spatially augmented LPBoosting for AD classification with evaluations on the ADNI dataset. *Neuroimage* 48, 138–149.
- Jack, C.R., Petersen, R.C., Xu, Y.C., O'Brien, P.C., Smith, G.E., Ivnik, R.J., Boeve, B.F., Waring, S.C., Tangalos, E., Kokmen, E., 1999. Prediction of AD with MRI-based hippocampal volume in mild cognitive impairment. *Neurology* 52, 1397–1403.
- Jack, C.R., Jr., Weigand, S.D., Shiung, M.M., Przybelski, S.A., O'Brien, P.C., Gunter, J.L., Knopman, D.S., Boeve, B.F., Smith, G.E., Petersen, R.C., 2008. Atrophy rates accelerate in amnesic mild cognitive impairment. *Neurology* 70, 1740–1752.
- Jack, C.R.J., Bernstein, M.A., Fox, N.C., Thompson, P., Alexander, G., Harvey, D., Borowski, B., Britson, P.J., Whitwell, J.L., Ward, C., Dale, A.M., Felmlee, J.P., Gunter, J.L., Hill, D.L., Killiany, R., Schuff, N., Fox-Bosetti, S., Lin, C., Studholme, C., deCarli, C.S., Krueger, G., Ward, H.A., Metzger, G.J., Scott, K.T., Mallozzi, R., Blezek, D., Levy,

- J., Debbins, J.P., Fleisher, A.S., Albert, M., Green, R., Bartzokis, G., Glover, G., Mugler, J., Weiner, M.W., 2008. The Alzheimer's disease neuroimaging initiative (ADNI): MRI methods. *J. Magn. Reson. Imaging* 27, 685–691.
- Kabani, N., MacDonald, D., Holmes, C.J., Evans, A., 1998. A 3D atlas of the human brain. *Neuroimage* 7, S717.
- Karas, G.B., Scheltens, P., Rombouts, S.A., Visser, P.J., van Schijndel, R.A., Fox, N.C., Barkhof, F., 2004. Global and local gray matter loss in mild cognitive impairment and Alzheimer's disease. *Neuroimage* 23, 708–716.
- Kaye, J., Swihart, T., Howieson, D., Dame, A., Moore, M., Karnos, T., Camicioli, R., Ball, M., Oken, B., Sexton, G., 1997. Volume loss of the hippocampus and temporal lobe in healthy elderly persons destined to develop dementia. *Neurology* 48, 1297–1304.
- Killiany, R.J., Gomez-Isla, T., Moss, M., Kikinis, R., Sandor, T., Jolesz, F., Tanzi, R., Jones, K., Hyman, B.T., Albert, M.S., 2000. Use of structural magnetic resonance imaging to predict who will get Alzheimer's disease Temporal lobe regions on magnetic resonance imaging identify patients with early Alzheimer's disease. *Ann. Neurol.* 47, 430–439.
- Kloppel, S., Stonnington, C.M., Chu, C., Draganski, B., Scahill, R.I., Rohrer, J.D., Fox, N.C., Jack, C.R., Jr, Ashburner, J., Frackowiak, R.S., 2008. Automatic classification of MR scans in Alzheimer's disease. *Brain* 131, 681–689.
- Lao, Z., Shen, D., Xue, Z., Karacali, B., Resnick, S.M., Davatzikos, C., 2004. Morphological classification of brains via high-dimensional shape transformations and machine learning methods. *Neuroimage* 21, 46–57.
- McEvoy, L.K., Fennema-Notestine, C., Roddey, J.C., Hagler, D.J., Jr, Holland, D., Karow, D.S., Pung, C.J., Brewer, J.B., Dale, A.M., 2009. Alzheimer disease: quantitative structural neuroimaging for detection and prediction of clinical and structural changes in mild cognitive impairment. *Radiology* 251, 195–205.
- Misra, C., Fan, Y., Davatzikos, C., 2009. Baseline and longitudinal patterns of brain atrophy in MCI patients, and their use in prediction of short-term conversion to AD: Results from ADNI. *Neuroimage* 44, 1415–1422.
- Pennanen, C., Testa, C., Laakso, M.P., Hallikainen, M., Helkala, E.L., Hanninen, T., Kivipelto, M., Kononen, M., Nissinen, A., Tervo, S., Vanhanen, M., Vanninen, R., Frisoni, G.B., Soininen, H., 2005. A voxel based morphometry study on mild cognitive impairment. *J. Neurol. Neurosurg. Psychiatry* 76, 11–14.
- Resnick, S.M., Pham, D.L., Kraut, M.A., Zonderman, A.B., Davatzikos, C., 2003. Longitudinal Magnetic Resonance Imaging Studies of Older Adults: A Shrinking Brain. *J. Neurosci.* 23, 295–301.
- Risacher, S.L., Saykin, A.J., West, J.D., Shen, L., Firpi, H.A., McDonald, B.C., 2009. Baseline MRI predictors of conversion from MCI to probable AD in the ADNI cohort. *Curr. Alzheimer Res.* 6, 347–361.
- Schneider, J.A., Wilson, R.S., Bienias, J.L., Evans, D.A., Bennett, D.A., 2004. Cerebral infarctions and the likelihood of dementia from Alzheimer disease pathology. *Neurology* 62, 1148–1155.
- Schuff, N., Woerner, N., Boreta, L., Kornfield, T., Shaw, L.M., Trojanowski, J.Q., Thompson, P.M., Jack, C.R., Jr, Weiner, M.W., 2009. MRI of hippocampal volume loss in early Alzheimer's disease in relation to ApoE genotype and biomarkers. *Brain* 132, 1067–1077.
- Shaw, L.M., Vanderstichele, H., Knapiak-Czajka, M., Clark, C.M., Aisen, P.S., Petersen, R.C., Blennow, K., Soares, H., Simon, A., Lewczuk, P., Dean, R., Siemers, E., Potter, W., Lee, V.M., Trojanowski, J.Q., 2009. Cerebrospinal fluid biomarker signature in Alzheimer's disease neuroimaging initiative subjects. *Ann. Neurol.* 65, 403–413.
- Stoub, T.R., Bulgakova, M., Leurgans, S., Bennett, D.A., Fleischman, D., Turner, D.A., deToledo-Morrell, L., 2005. MRI predictors of risk of incident Alzheimer disease: A longitudinal study. *Neurology* 64, 1520–1524.
- Thompson, P., Hayashi, K., Dutton, R., Chiang, M., Leow, A., Sowell, E., De Zubicaray, G., Becker, J., Lopez, O., Aizenstein, H., Toga, A., 2007. Tracking Alzheimer's disease. *Ann. N Y Acad. Sci.* 1097, 183–214.
- Vapnik, V.N., 1998. *Statistical Learning Theory*. Wiley, New York.
- Vemuri, P., Wiste, H.J., Weigand, S.D., Shaw, L.M., Trojanowski, J.Q., Weiner, M.W., Knopman, D.S., Petersen, R.C., Jack, C.R., Jr, Alzheimer's Disease Neuroimaging Initiative, 2009. MRI and CSF biomarkers in normal, MCI, and AD subjects: Predicting future clinical changes. *Neurology* 73, 294–301.
- Visser, P.J., Verhey, F.R., Hofman, P.A., Scheltens, P., Jolles, J., 2002. Medial temporal lobe atrophy predicts Alzheimer's disease in patients with minor cognitive impairment. *J. Neurol. Neurosurg. Psychiatry* 72, 491–497.